African Easterly Waves in 30-day High-resolution Global Simulations: A Case Study during the NAMMA Period in 2006

Bo-Wen Shen[1,2] and others

[1]UMCP/ESSIC, [2]NASA/GSFC

Abstract

In August 2006, the NASA African Monsoon Multidisciplinary Analyses (NAMMA) field campaign was launched, providing great opportunities to characterize the frequency of African Easterly Waves (AEWs) and evolution of their structure over continental western Africa. In this study, extended-range (30day) high-resolution simulations with the NASA global mesoscale model are conducted to examine model's ability to simulate the initiation and propagation of six consecutive AEWs and African Easterly Jet (AEJ) from late August to September, 2006 and their modulation on hurricane formation. By comparing simulations with NAMMA observations and NCEP reanalysis, we will show that the statistic characteristics of individual AEWs are realistically simulated with larger errors in 5th and 6th AEWs. In addition, remarkable simulations of an AEJ averaged over the entire 30 days are also obtained. Nine additional 30-day simulations with different dynamic initial conditions (ICs) and land surface ICs suggest that though land surface processes might contribute to the predictability of the AEJ and AEWs, initiation and detailed evolution of AEWs still depend on accurate representation of dynamic and land surface ICs and their nonlinear interactions. More interestingly, our results show a potential of extending the lead time of hurricane formation prediction (e.g., with a lead time up to 22 days) as the initiation and evolution of the 4th AEW and its interactions with local environments (e.g., Guinea Highlands) are accurately simulated.

Key words: AEW, hurricane forecast, global mesoscale model, supercomputing

1. Introduction

Extending the lead time of hurricane prediction is important for saving lives and reducing damage, but is very difficult with numerical models. Though global models have been used to study hurricane climate, further improvement in increasing the accuracy of simulating the timing and location for hurricanes is still desired. Recent advance in high-resolution global models and supercomputing technology has shown a potential for achieving this. A challenging question to be answered is: under what kind of conditions the lead time of predicted mesoscale hurricane can be extended?

It has been suggested that hurricane activities can be modulated by large-scale flows such as AEWs, implying that accurate representations of an initial AEW and simulations of AEW initiation and subsequent evolution may contribute to the improvement of hurricane formation prediction. Being characterized by an average westward-propagating speed of 11.6 m/s, an average wavelength of 2000~4000km, and a period of about 2 to 5 days, AEWs appear as one of the dominant synoptic weather systems in West Africa during the summer time (from June to early October). Previous studies showed that some AEWs could develop into hurricanes in the Atlantic and even East Pacific regions (e.g., Carlson, 1969) and that nearly 85% of intense hurricanes have their origins as AEWs (e.g., Landsea, 1993).

The initiation of an AEW is found to be related to the release of barotropic and/or baroclinic instability associated with an African Easterly Jet (AEJ), and the maintenance of the AEJ could be replenished by diabatically forced meridional circulations associated with Saharan heat low region and ITCZ (Thorncroft and Blackburn, 1999). While AEWs could modulate the features of the the Inter-Tropical Discontinuity (ITD), where the African northeasterly trade winds and southwesterly monsoon flows meet (e.g., Berry and Thorncroft, 2005 and references therein), the diabatic heating associated with the ITD over the African continent may further initiate AEWs. To this end, recent studies suggest view the AEWs and AEJ as an integrated system in order to improve understanding of their interactions with surface processes and diabatic convection (e.g., Cornforth et al., 2009). Along with this view, to extend the lead time of predicting this kind of hurricanes near the Cape Verde islands, it is important to accurately simulate the multiscale interactions among hurricanes, AEWs, and AEJ, and surface mechanic and thermal processes.

The NASA African Monsoon Multidisciplinary Analyses (NAMMA) field campaign was launched in August 2006, which provides great opportunities to characterize the frequency of AEWs, their evolution over continental western Africa, and their impacts on regional water and energy budgets. During the 30-day observation period between late August and late September, it has been documented that there were six AEWs appearing (in eastern Africa), propagating westward, and passing by the Cape Verde Islands, 350 miles off the west coast of Africa. During this period, the formation of Hurricane

Helene (2006) in early September is found to be related to the interaction between an observed AEW and local environments. In this study, the NAMMA observations and NCEP reanalysis are used to examine the multiscale interactions of simulated AEWs with the aim of addressing the following questions: (1) if and how extended-range simulations of AEWs can be improved with a high-resolution global model; (2) to what extent large-scale flows such as an AEW could determine the timing and location of TC genesis (e.g., Helene in this study).

2. The Model and Numerical Approach

The global mesoscale model (also known as the high-resolution finite-volume GCM; fvGCM) is composed of three major components: 1) finite-volume dynamics, 2) NCAR CCM3 physics, and 3) the NCAR Community Land model (Lin 2004; Atlas et al. 2005; Shen et al. 2006). In this study, the 0.25^o model with a large-scale condensation scheme (e.g., Shen et al., 2010) is used for performing experiments. Dynamic initial conditions (ICs) and sea surface temperatures (SSTs) are derived from Global Forecast System (GFS) T384 (~ 35km) analysis data and 1° optimum interpolation SSTs from the National Centers for Environmental Prediction (NCEP). In previous studies by other researchers, soil moisture (e.g., Hsieh and Cook, 2005) or meridional surface temperature gradient (Cornforth et al., 2009) is prescribed. To generate land surface (and physics) ICs to be consistent with the dynamic ICs, we have performed more than 2-year warm-start runs.

3. Numerical Results

In the following, we first verify 30-day high-resolution simulations initialized at 0000 UTC August 22, 2009 against the NCEP Reanalysis, and then discuss sensitivity experiments to understand the impacts of different dynamics ICs, land surface ICs and surface boundary conditions (e.g., SSTs) on the simulations of AEWs and AEJ. We will also discuss the modulation of Helene's formation by one of the AEWs.

3.1 AEWs and AEJ in the 30-day Control Run

Fig. 1 shows NCEP 2.5^o reanalysis (top panels) and 0.25^o simulations (bottom panels) during the period of between August 22 and September 21, 2006. The time/longitude profile of meridional winds averaged over 5° to 20°N is shown in Fig. 1a and 1d. During this 30-day period, both model simulations and reanalysis indicate the occurrence of six westward propagating signals, which can be identified as AEWs. These waves have a time scale of 3~5 days, a wavelength of about 2000-2500km, and a propagating speed of about 10m/s. Overall, model simulations are in good agreement with the reanalysis, in particular over the Africa continent. Spatial and temporal variations exist but are within one characteristic (time and spatial) scale. It should be noted

that strong wind shear along 20°W during 11-13 September, as shown by a black circle in Fig. 1d, indicates the formation of hurricane Helene (2006).

Figs. 1b and 1e display the altitude/latitude cross section of zonal winds averaged over the 30-day period along longitude 10°E. A low-level jet with maximum of around 10~14 m/s at (14°N, 600 hPa) is clearly shown in both model simulations and reanalysis. A jet with these features over the Africa during the northern hemisphere summer is called the AEJ (Thorncroft and Blackburn, 1999). At about 200hPa and equatorward of the AEJ, the model simulates an upper-level tropical easterly jet (TEJ), which appears at a right height but has stronger intensity between 9°N and 15°N. Below and south of the AEJ, a low-level monsoon westerly flow is simulated (Fig. 1e), and compared well with the NCEP reanalysis (Fig. 1b). Fig. 1c and 1f shows the same fields but along longitude 20°E. Overall, the model simulation is in good agreement with the NCEP reanalysis, but the simulated AEJ is slightly weaker.

Fig. 2a (Fig. 2b) shows the spatial distribution of 600-hPa zonal winds (850-hPa temperatures) averaged over the entire 30 days for NCEP reanalysis, and Fig. 2c (2d) for model simulations. Overall, winds and temperatures are simulated realistically with respect to the analysis. The simulated 600-hPa AEJ along latitude 15°N is weaker (e.g., in the area of 10°W-5°E and 15°-25°N), and it extends less westward and northward than the one in the reanalysis. The maintenance of the AEJ could be replenished by the diabatically meridional circulation which is dependent of the distribution of the surface temperature. Thus, as shown in the Figs. (b) and (d), a good agreement between the simulated 850-hPa temperature and the reanalysis provides a good opportunity of verifying the role of the meridional circulation on the evolution of the AEJ, which is the subject for a further study.

3.2 Sensitivity Experiments

From a numerical modeling perspective, accurate ICs and sophisticated model dynamics (e.g., grid spacing), physics (e.g., parameterizations) and land surface processes are important for the accurate simulations of the multiscale flows and their interactions. It is known that a short-term forecast is classified as an initial value problem, and a long-term (seasonal or longer) forecast as a boundary value problem. To examine the sensitivity of extended AEW simulations on different ICs and BCs, we conduct 9 additional experiments (1) by initializing the model with three different dynamic ICs at 0000 UTC for three consecutive days, (2) by applying different land surface ICs (used by the land model), or replacing weekly SSTs with climate SSTs, and (3) by using the the same physics and land surface ICs as those in the control run but using a dynamic IC in a different season (e.g., 22 April and 22 June 2006) , and (4) by reducing the height of the Guinea Highlands. Table 1 gives a summary on these experiments.

In each of the 9 experiments, its time/longitude cross section of meridional winds averaged over latitudes 5°N-20°N is shown in Fig. 3(a)-(i), respectively. Panels (a)-(c) show the simulations initialized at 0000 UTC from Aug. 23-25. As the characteristic time scale of AEWs is about 3~5 days, the period of Aug. 22-25 cover a different phase of the initial (the 1st) AEW. Overall, initiation and propagation of the AEWs in the three experiments are simulated comparably, though variations exist within one characteristic scale. However, the impact of the different ICs (e.g., the phase difference in the initial AEW) on the successive initiation of AEWs and their modulation on hurricane formation is still desired but beyond the scope of this study.

Land surface processes may be important for the maintenance of the AEJ and thus for the initiation of AEWs. Panel (d) shows model results initialized with the same dynamic and physics ICs but with a land surface IC from a cold start run. This run simulates the evolution of the initial AEW with satisfaction up to 8~9 days, but fails to simulate the initiation of any "realistic" AEWs. In comparison, Case E (in Fig 3e), which uses a land surface IC derived from a previous run on 22 June can realistically capture the initiations of AEWs over land. However, larger (timing) errors appear in the 4th, 5th, and 6th AEWs, and weaker downstream development over the ocean (e.g., for the 4th AEW) is observed. In comparison with the land surface processes, the oceanic processes on the extended range simulations of AEWs is investigated with a simple experiment by replacing the weekly SSTs with the climate SSTs. This run (Fig. 3f) shows that the evolution of the first four AEWs is comparable to those in the control run. Differences appear in the 5th and 6th AEWs, showing that the effects of using climate SSTs on the simulation of AEW initiation become effective after 15~20-day integration, presuming that synoptic-scale environmental flows were first changed and then impacted the AEW initiation.

The above three experiments focus on the surface processes (as low-level BCs). The next two experiments are designed to examine the impact of different dynamic ICs in a different month. With the same physics and land surface ICs, Cases G and H are performed with the dynamic ICs on 22 April and June, respectively, of which timestamps are changed to 22 Aug in order to keep the same model physics (e.g., radiation) and land model configurations as the control run. As shown in Fig. 3g, the run with the dynamic IC in the Spring cannot simulate any realistic AEW signals. In comparison, the run with the IC on 22 June is able to simulate AEW signals with some degree of satisfaction. However, large discrepancy in timing and location exists.

The last experiment is used to examine the mechanic effects of Guinea Highlands on the simulations of AEWs (e.g., the 4th AEW) by multiplying a factor of 0.6 to the mountain heights, which can mimic the effects of less accurate mountain heights in a coarse-resolution model. Fig. 3i shows that initiation of the 4th, 5th and 6th AEWs are influenced by this change, and the downstream

development of AEWs (e.g., the 2nd and 4th AEWs) becomes weaker.

3.3. Modulation on Hurricane Genesis

The altitude/time cross section of meridional winds at (23.5°W, 14.9°N) is shown in Fig. 4a-c for NMMA observations, NCEP 2.5° reanalysis and 0.25° model results, respectively. For comparison, the model results are averaged over a 2° box. In general, the timing and location of maximum southerly winds (indicated by a yellow color) from the model is quite close to those from NAMMA observations and NCEP reanalysis except that an additional signal appears on about 08/31. This false-positive event is stronger than the one in NCEP reanalysis, and has a time lag of about 1 day.

Observation showed that the 4th AEW on Sep 13 developed into Hurricane Helene (2006). Fig. 5a shows the movement of the model Helene after its formation in the simulation, as compared to the best track. The initial location of Helen is predicted remarkably at Day 22 with a displace error of 300 km. The subsequent movement from day 22 to day 30 is quite realistic with the largest error of about 700 km on Sep. 19 (at Day 28). Helene intensified slowly before Sep. 15, and experienced rapid intensification (RI) between Sep. 15-18, and maintained its strength during Sep. 18-21. The intensity evolution is realistically simulated with a time lag of only 1-2 days, as shown in Figure 5b. Our run not only simulates the RI stage but also the maintenance stage between Day 28 and 30.

4. Concluding Remarks:

In this study, we conduct ten 30-day 0.25° simulations with the NASA global mesoscale model to understand the model ability in simulating the initiations and propagation of 6 consecutive AEWs in late August 2006, and the mean state of the AEJ over the Africa and the downstream in the tropical Atlantic, aimed at extending the lead time of hurricane formation prediction near the Cape Verde Island.

The control run initialized at 0000 UTC 22 August 2006 is first discussed. During this period, 6 AEWs and time-averaged AEJ are realistically simulated except that the simulated 5th and 6th AEWs have relatively larger errors in timing, as compared to NCEP reanalysis and NAMMA observations. In addition, a mesoscale vortex appears in the 22-day integration, and develops into a hurricane as numerical integration proceeds. This simulated mesoscale vortex resembles the observed Hurricane Helene with respect to the genesis timing, location and initial intensity, and also to the subsequent movement and intensification.

Nine additional 30-days experiments (e.g., with different dynamic ICs and land surface ICs) collectively suggest (1) that accurate representations of non-linear interactions between atmosphere and land processes are crucial for improving extended-range simulations of AEWs (e.g., consecutive initiation of AEWs) and AEJ;

(2) that improved simulations of an individual AEW and its interaction with local environments (e.g., Guinea Highlands) could provide determinism for the hurricane formation in the downstream (e.g., Helene) and thus extend the lead of formation prediction; (3) however, the dependence of AEW simulations on accurate dynamic and surface ICs and BCs poses a challenge in simulating their modulation on hurricane activities. Further analyses are still desired to examine model's performance in simulating energy conversion among the AEJ and individual AEWs and meridional circulations. In addition, we still need to understand critical processes that lead to the development of an AEW into a hurricane.

A recent trend to understand the tropical cyclogenesis processes is to examine the role of the critical layer/level (CL) associated with a tropical easterly wave (Dunkerton et al., 2008). Though CL dynamics have been studied with idealized models extensively, it is still challenging to examine its role in weather prediction models. Among the challenges are determining the propagation (or phase) speed of the "wave" and increasing grid spacing to resolve the CL accurately. In addition to the "classical" CL, different types of CLs may exist, including inertia CLs associated with the inclusion of the Coriolis force, and Rossby CLs (e.g., Shen and Lin, 1999). Depending on the relative importance of environmental factors such as static stability, vertical wind shear and the Coriolis force, a CL my absorb, reflect or over-reflect the energy of approaching disturbances. Thus, the efficiency of energy absorption/reflection by the resolved CL in numerical models needs to be examined carefully to understand its impact on hurricane formation, which is the subject for a further study.

Acknowledgments:

References:

Atlas, R., et al. 2005, Hurricane forecasting with the high-resolution NASA finite volume general circulation model. *Geophys. Res. Lett.,* **32**, L03801, doi:10.1029/2004GL021513.

Berry, G. J., and C. Thorncroft, 2005: Case Study on an Intense African Easterly Wave. *Mon. Wea. Rev.*, **133**, 752-766.

Carlson, T. N., 1969: Synoptic histories of three Africa disturbances that developed into Atlantic hurricanes. *Mon. Wea. Rev.,* **97**, 256-276.

Cornforth, R. J., B. J. Hoskins, and C. D. Thorncroft, 2009: The Impact of Moist Processes on the African Easterly Jet-African Easterly Wave System. *Q.J.R. Meteorol. Soc.,* **135**, 894-913.

Dunkerton, T. J., M. T. Montgomery, and Z. Wang, 2008: Tropical Cyclogenesis in a Tropical Wave Critical Layer: Easterly Waves. *Atmos. Chem. Phys. Discuss.* **8**, 11149-11292.

Hsieh, J.-S., and K. H. Cook, 2005: Generation of African Easterly Wave Disturbance: Relationship to the African Easterly Jet. *Mon. Wea. Rev.,* **133**, 1311-1327.

Landsea, C.W. (1993): A climatology of intense (or major) Atlantic hurricanes. *Mon. Wea. Rev.,* **121**, 1703-1713.

Lin, S.-J., 2004: A vertically Lagrangian finite-volume dynamical core for global models. *Mon. Wea. Rev.*, **132**, 2293-2307.

Schmidlin, F. J., B. Morrison, T. Baldwin, E. T. Northam, 2007: High Resolution Radiosonde Measurements from Cape Verde: Details of Easterly Wave Passage. AGU 2007 Fall Meeting.

Shen, B.- W., and Y.-L. Lin, 1999: Effects of Critical Levels on Two-Dimensional Backsheared Flow over an Isolated Mountain Ridge on an f-plane. *J. of Atmos. Sci.,* **56**, 3286-3302.

Shen, B.-W., et al. 2006: Hurricane forecasts with a global mesoscale-resolving model on the NASA Columbia supercomputer. *Geophys. Res. Lett.*, **33**, L, doi:10.1029/2006GL026143.

Shen, B.-W., W.-K. Tao, W. K. Lau, R. Atlas, 2010: Predicting Tropical Cyclogenesis with a Global Mesoscale Model: Hierarchical Multiscale Interactions During the Formation of Tropical Cyclone Nargis (2008) . *J. Geophys. Res.*, doi:10.1029/2009JD013140.

Thorncroft, C. D. and M. Blackburn, 1999: Maintenance of the African easterly jet. *QJMS*, **125**, 763-786.

Table 1: Sensitivity experiments for examining the dependence of AEW simulations on different dynamic ICs, different land surface ICs, different SST and modified Guinea Highlands with a reduced height.

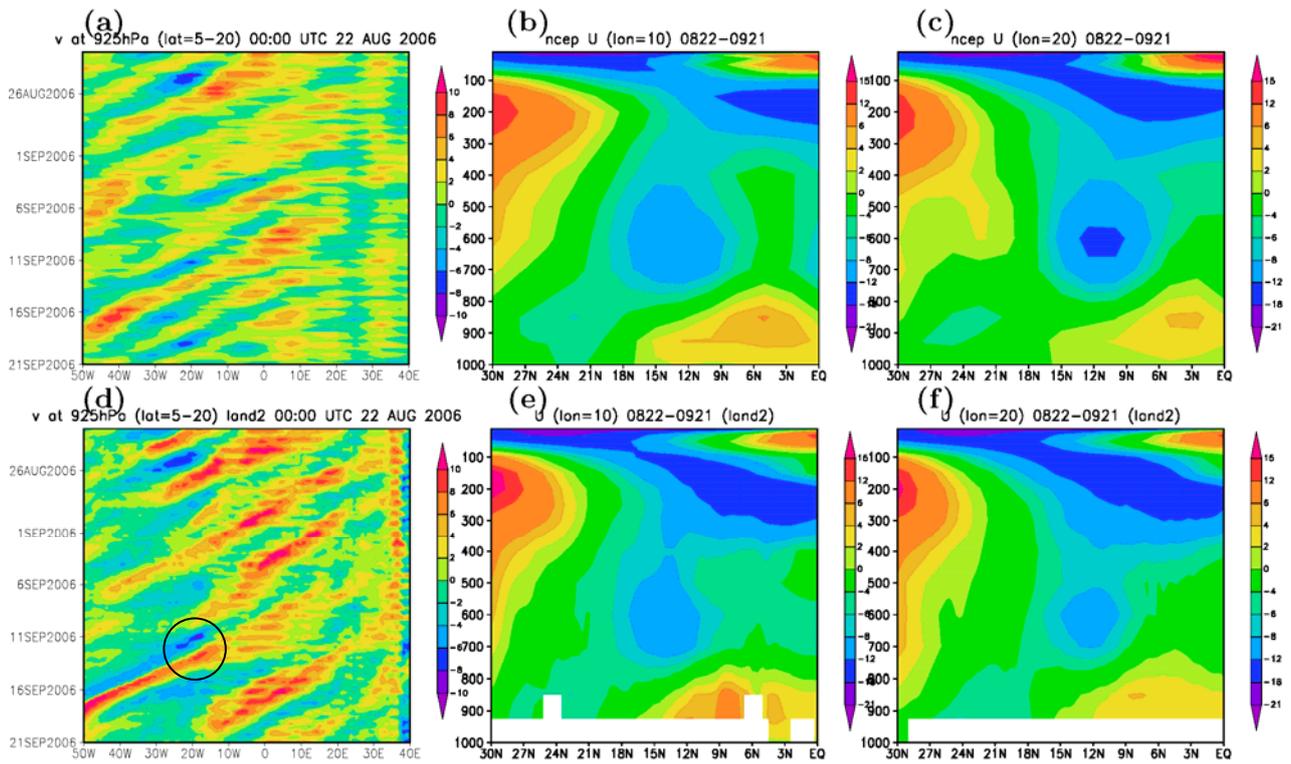| Case id	Dynamic IC	land surface IC	SST	Guinea Highlands	Remarks
cntl	08/22	08/22	weekly		
A	08/23	08/23	weekly		
B	08/24	08/24	weekly		
C	08/25	08/25	weekly		
D	08/22	cold-start	weekly		
E	08/22	02/22	weekly		
F	08/22	08/22	climate		
G	04/22	08/22	weekly		date changed to be 08/22/2006
H	06/22	08/22	weekly		date changed to be 08/22/2006
I	08/22	08/22	weekly	A factor of 0.6 in heights	

Figure 1: Six AEWs and AEJ in GFS analysis data (top panels) and a 30-day simulation (bottom panels) initialized at 0000 UTC August 22, 2006 with the global mesoscale model. Left panels (a,d): time-longitude diagram of meridional winds averaged over latitudes of 5-20°N from 22 August to 21 September, 2006. Right panels: height-latitude cross section of time-averaged zonal winds along the longitude 10°E (b,e) and 20°E (c,f), respectively. A black circle in Fig. 1d roughly indicates the timing and location of the Helene's formation.
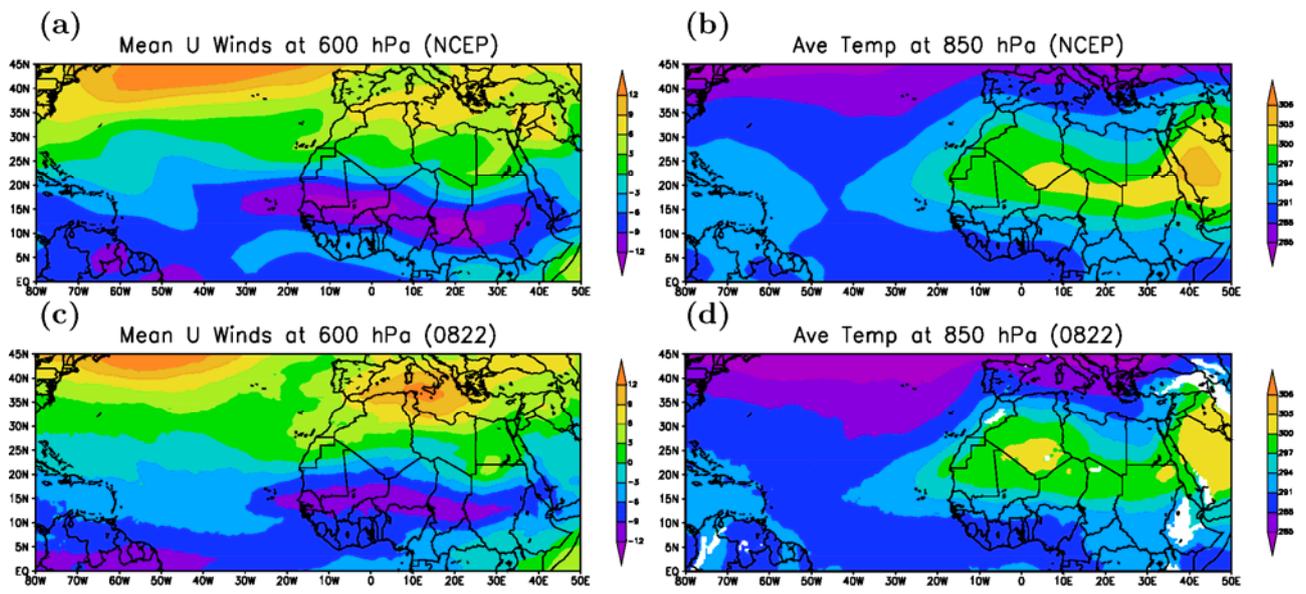
Figure 2: 30-day averaged fields from GFS reanalysis (top) and model simulations (bottom). Panels (a,c) are averaged zonal winds (m/s) at 600 hPa, and Panels (b,d) temperatures (^{o}C) at 850 hPa.
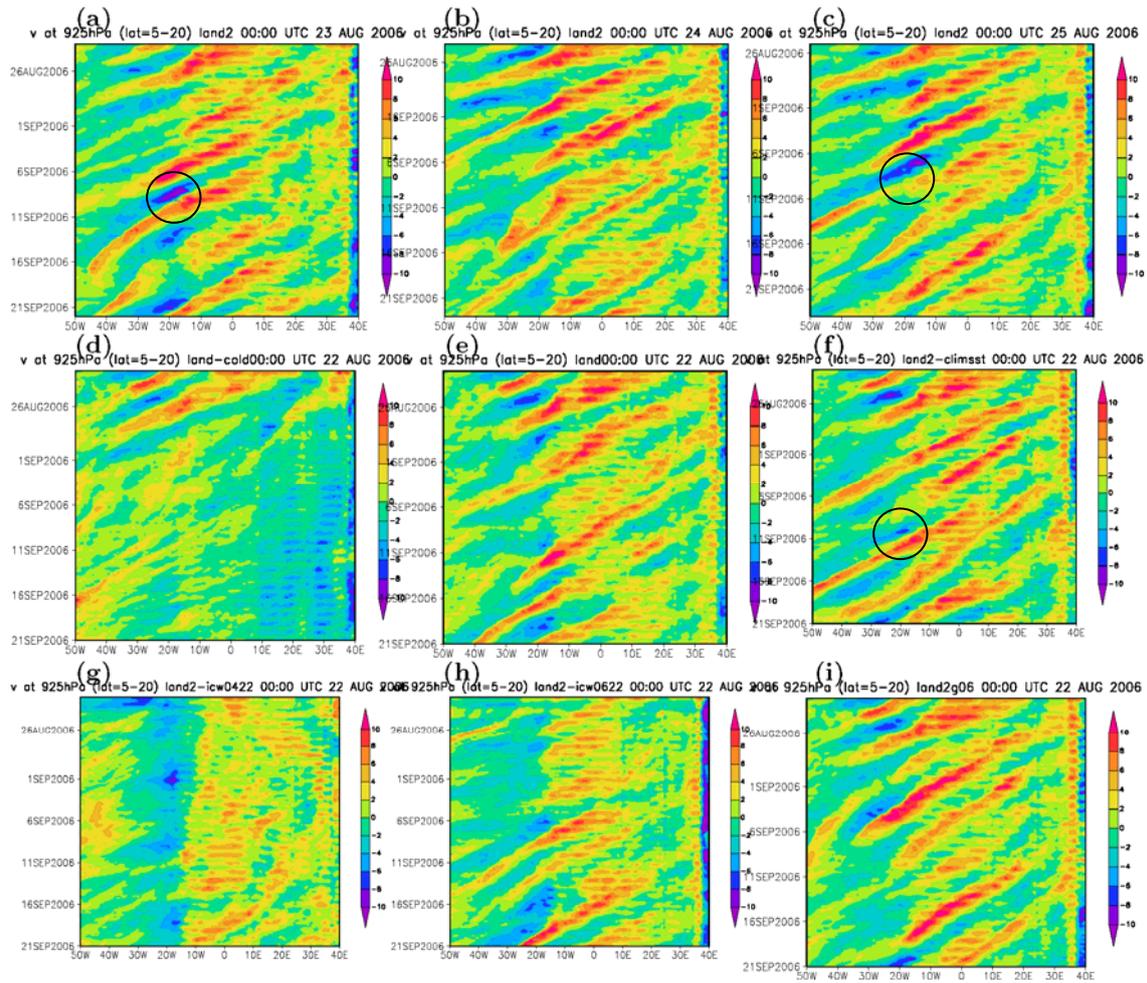
Figure 3: Sensitivity of AEW simulations on different dynamic ICs, land surface ICs, different SSTs, and Guinea Highland with a reduced height. Panels (a)-(i) are simulated meridional winds from Cases (A)-(I) listed in Table 1.
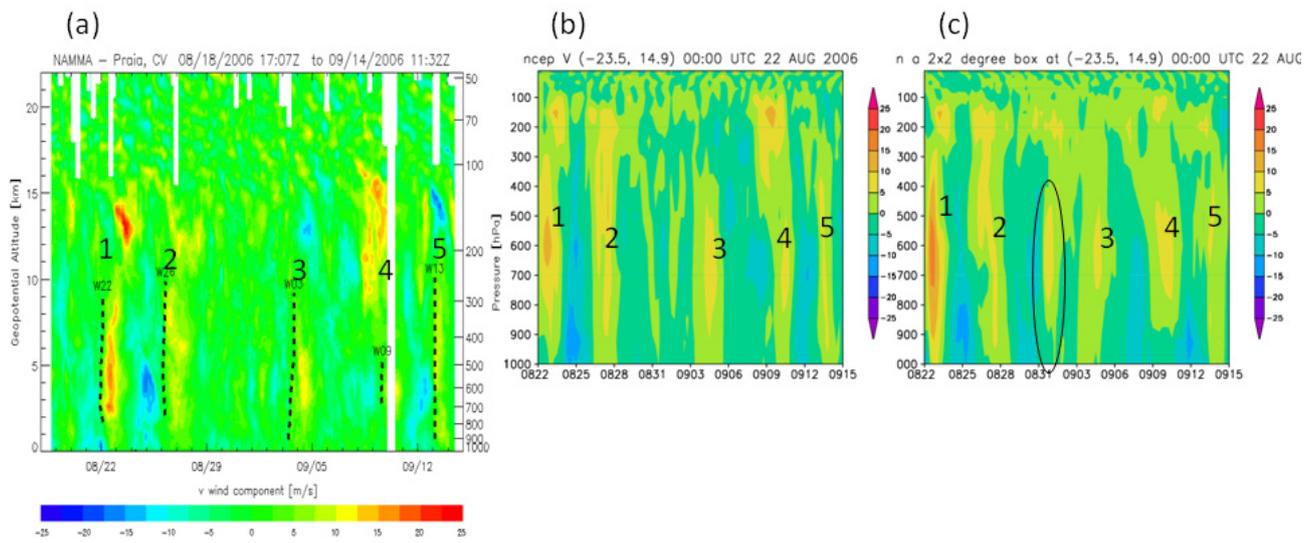
Figure 4: Altitude-time cross section of meridional winds at (23.5^{o}E, 14.9^o N) from NAMMA observation (a, Schmidlin et al., 2007), GFS reanalysis (b) and model simulation averaged over a 2°x2^o box (c).
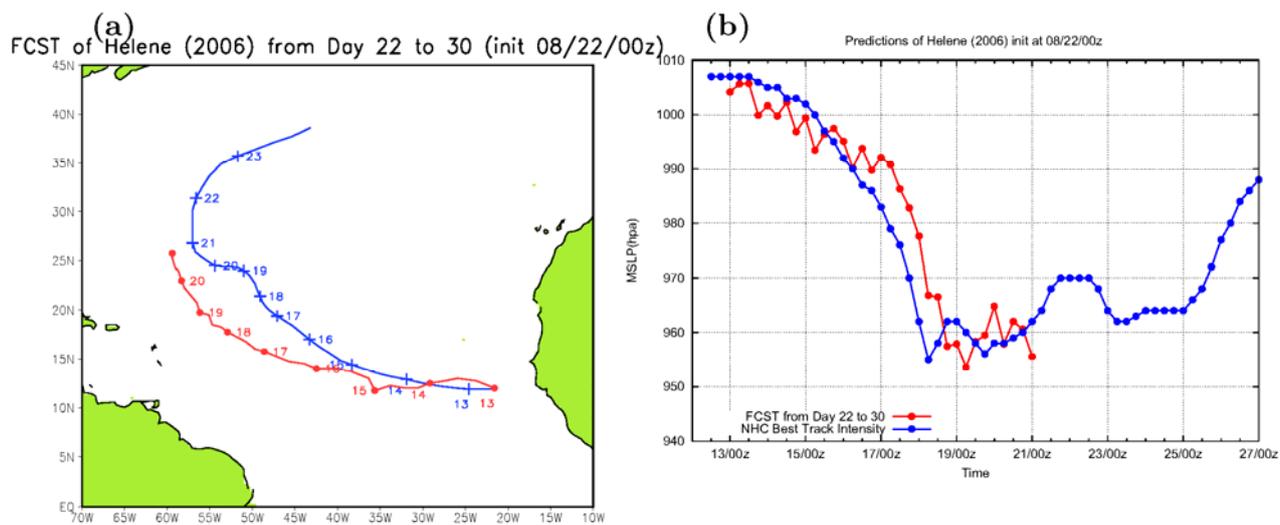
Figure 5: Track (a) and intensity (b) forecasts for Hurricane Helene (2006) from Day 22 to 30. Red and blue lines indicate model predictions and best tracks, respectively.